




REGULAR ARTICLE

Reactive Sintering of HfB<sub>2</sub>-SiC-C Ultra-High Temperature Ceramics with Enhanced Thermal Shock Resistance

A. Ovcharenko\* , V. Dibrov, M. Semenko 

Taras Shevchenko National University of Kyiv, 01601 Kyiv, Ukraine

(Received 15 October 2024; revised manuscript received 20 December 2024; published online 23 December 2024)

The fabrication of ultra-high-temperature ceramics using the sintering method requires maintaining high temperatures of around 1500 °C for several hours. In contrast, this study demonstrated an alternative method for uniform formation of the corresponding microphases, which could reduce production costs in the future. The essence of the reactive hot pressing method lies in initiating a chemical reaction at an adiabatic temperature, which constitutes 60-80 % of the precursors' melting temperature, with the application of external pressure. The combination of these conditions significantly accelerates the densification process of the powder batch. The HfB<sub>2</sub>-SiC-C heteromodulus ceramics with different content of carbon platelets were manufactured via the reactive hot pressing of HfC-B<sub>4</sub>C-Si precursors at 1850 °C and 30 MPa for 4 minutes. Thus, the microhardness of the synthesized ceramics with specific chemical compositions reached 17.3 GPa, while the fracture toughness was 6.9 MPa/m<sup>2</sup>. The reactively pressed materials were compared to non-reactively pressed ones with the same compositions. X-Ray Diffraction (XRD) and Scanning Electron Microscopy (SEM) have been used for the composite characterization. Carbon inclusions were shown affecting the HfB<sub>2</sub>-SiC hardness while improving thermal shock resistance. The stratification of reactively pressed materials has been identified with silicon-depleted inner areas of the samples.

**Keywords:** Ultra-high temperature ceramics, Reactive sintering, Hafnium diboride, Thermal shock resistance, XRD, SEM.

DOI: [10.21272/jnep.16\(6\).06024](https://doi.org/10.21272/jnep.16(6).06024)

PACS numbers: 81.05.Je, 81.05.Mh

1. INTRODUCTION

Ultra-high temperature ceramics (UHTCs), are materials known for their extremely high melting points, often exceeding 3000 °C. However, the practical definition emphasizes that UHTCs are ceramic materials that maintain structural integrity during prolonged periods at temperatures higher than 1650 °C. UHTCs appear to be promising for critical structural parts of rockets and hypersonic vehicles, including nozzles, leading edges, and engine components [1-4].

Ceramics based on ZrB<sub>2</sub> and especially HfB<sub>2</sub> have outstanding properties even for UHTCs. They have high melting temperatures, high strength, chemical resistance, high physical stability (due to the absence of phase transformations), thermal conductivity, and the ability to retain strength at elevated temperatures [5-6]. Several recent papers pointed out that the main areas of research interest for those materials were sintering, mechanical properties, compound modifications, and degradation of materials at higher temperatures [7-9].

Hf/ZrB<sub>2</sub>-SiC-based materials offer potential advantages [10] in terms of high-temperature stability. However, there are two significant challenges in their manufacturing and application. First, while presenting a clear advantage over other structural ceramics available in terms of thermal shock resistance (TSR), the measured temperature difference of failure of about 400 °C is well

below what may be encountered in proposed applications [11]. Second, a noticeable disadvantage is the need for high sintering temperatures [12]. Usually, sintering additives are used to lower the processing parameters. However, such additives would inevitably affect the high-temperature characteristics.

Several efficient strategies have been applied to significantly increase the TSR and fracture toughness of HfB<sub>2</sub>/ZrB<sub>2</sub>-SiC-based composites, as well as to lower their sintering temperature, including:

- Incorporating whisker-like SiC, which requires lower sintering temperatures [13].
- Stimulation of on-site formation of prolonged Hf/ZrB<sub>2</sub> or SiC grains [14].
- Using a laminated structure to create residual compressive stresses. These improved mechanical properties are attributed to residual stresses resulting from the thermoelastic mismatch between adjacent layers [15].
- Introduction of weak interfaces that redirect propagating cracks. This increased the fracture toughness by approximately 41 % compared to the reference material [16].

Reactive hot pressing (RHP) emerges as a promising way to address the obstacles of elevated processing temperature and time [17-20]. During RHP, the targeted composite phases originate from chemical reactions among the initial components with low melting points [21-23], facilitating material densification. This method

\* Correspondence e-mail: [terra.2016knu@gmail.com](mailto:terra.2016knu@gmail.com)



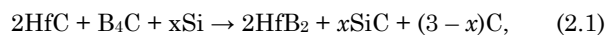
mitigates the necessity for high temperatures and extended processing durations and obviates the need for sintering aids [24].

Popov et al. used the technique to sinter similar  $ZrB_2$ -SiC| $ZrB_2$ -SiC-CNT| $TiB_2$ -SiC-CNT UTHC composite systems by reactive hot pressing of MeC-B<sub>4</sub>C-Si precursor powders. Full densification and enhanced thermomechanical properties of targeted materials were acquired [12, 22]. The presented paper demonstrates the use of the mentioned reactive sintering approach to facilitate the HfB<sub>2</sub>-SiC-C UHTCs manufacturing.

## 2. EXPERIMENTAL PROCEDURE

Commercially available powders of HfC (~ 70 μm), B<sub>4</sub>C (~ 20 μm) and Si (~ 20 μm) (Donetsk Reactive Factory, Ukraine) were used as green body materials. As stated by the manufacturers, the material purity was around 99.0 at %.

The material compositions were chosen according to the left-hand side of the following equation:



with  $x = 0; 0.5; 1; 1.5; 2.5$  (samples 1-5, Table 1).

To compare the manufacturing process and mechanical characteristics, the reference (non-reactively sintered) samples were hot-pressed based on the right-hand side of the reaction (1) with  $x = 0; 1.5; 2.5$  (samples N1, N4, and N5, Table 2).

**Table 1** – The initial powder composition of the reactively pressed samples

Sample #	Initial powders		
	HfC, wt.%	B <sub>4</sub> C, wt.%	Si, wt.%
1	87.3	12.7	0
2	84.6	12.3	3.1
3	82.1	11.9	6
4	79.7	11.5	8.8
5	75.3	10.9	13.8

**Table 2** – The initial powder composition of non-reactively pressed samples

Sample #	Initial powders		
	HfB <sub>2</sub> , wt.%	SiC, wt.%	C, wt.%
N1	91.74	0	8.26
N4	83.66	12.57	3.77
N5	79.02	19.79	1.18

The green body materials were prepared by grinding in a planetary mill in a zirconia jar with 10 mm zirconia balls (ball to powder ratio 10:1) at 1200 r.p.m. for 30 min. The milled powder average grain size approximated 10 μm.

All the samples were hot pressed at 1850 °C and 30 MPa for 4 minutes in a graphite mould with no vacuum or any special protective atmosphere in a hot pressing furnace with resistive heating created at Taras Shevchenko National University of Kyiv, Faculty of Physics, Metal Physics Department (Kyiv, Ukraine) [25]. The heating rate (after pre-heating at 600 °C for 15 min) was approximately 70 °C/min.

Hexagonal boron nitride powder was applied to the inner surface of the mould in order to prevent the formation of strong adhesion of the samples to the graphite matrix during the hot pressing.

After cooling, the samples were subjected to the following mechanical processing. First, the surface layer enriched with graphite and boron nitride, up to 1 mm thick, was removed using grinding wheels. Then, the surface of the sample was polished using diamond pastes with a dispersion of 10, 5 – 3, and 1 μm.

The density of the samples was determined using Archimedes' method.

The hardness of the sintered materials was measured by the Vickers indenter with a PMT-3 device with a load of 57 N for 10 s. The fracture toughness was estimated by measuring the crack lengths generated by the Vickers indentations with a load of 57 N. The toughness was calculated according to the formula of Evans and Charles [26].

The crystalline phases were identified by X-ray diffraction (XRD) and the identification was supported by Scanning Electron Microscopy (SEM). For the SEM analysis, ceramic samples were cleaved, allowing to avoid polishing artefacts in a composite with phases with a high hardness difference.

The thermal shock resistance was measured according to the indentation-quench method using the Therm-1 device [27]. The samples were heated to a preselected set of temperatures: 100, 225, 300, 350, 400, 450, 500, 600 and 700 °C for 10 minutes and then quenched in a water bath at room temperature (20 °C). The radial crack lengths of each indentation were measured before and after each quenching event by an optical microscope. The crack growth was expressed as a percentage to the initial crack length as:

$$(c_i - c_0)/c_0 \times 100 \% \quad (2.2)$$

with  $i$  being the number of the consequent quenching procedure. The average crack growth for each material was estimated as a function of the temperature interval.

## 3. EXPERIMENTAL RESULTS AND DISCUSSION

The X-ray diffractometry presented in Fig. 1 confirms the reaction (2.1) completion during the hot-pressing procedure.

Time dependencies of the green body height and the process temperature are presented in Fig. 2, showing significant differences between the reactive and non-reactive densification kinetics. The RHP shrinkage (Fig. 2 a) consists of two waves. According to [12], the first wave starting at 1250 °C reflects the reaction (1) initiation and corresponding powder mobility enhancement. The second wave observed after the system reaches a temperature of 1500 °C shows the new-formed crystal plastic deformation.

The absence of the first wave in the reaction-free process (Fig. 2b) further confirms its reaction-derived nature. The non-reactive densification starts at a temperature of about 1450-1500 °C and progresses with lower speed. The density and mechanical characteristics of the manufactured materials are presented in Table 3.

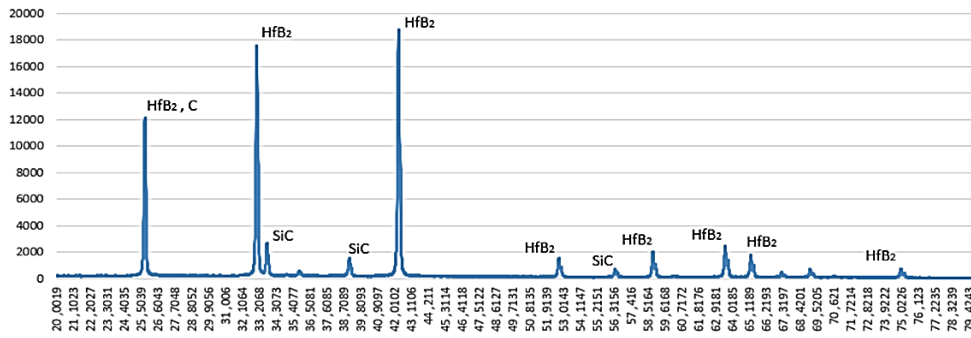


Fig. 1 – The X-ray diffraction of sample 2 after sintering

Significant differences in the density of reactively and non-reactively sintered samples of the equivalent compositions show the perspectives of the reactive hot pressing procedure for HfB<sub>2</sub>-SiC-based material manufacturing. Both hardness and toughness decrease with the graphite content, with H<sub>v</sub> being, in general, higher for reactively-pressed samples.

However, the materials thermal shock resistance (TSR) increases significantly with graphite content (See Fig. 3): samples with 29 vol.% of the soft phase inclusions withstood quenching from 700 °C, while sample 5 (4 vol.% of graphite) started deteriorating after 300 °C. The behaviour of similar composites was explained in [19] with  $R''$  criterion presented by Lu and Fleck [28]:

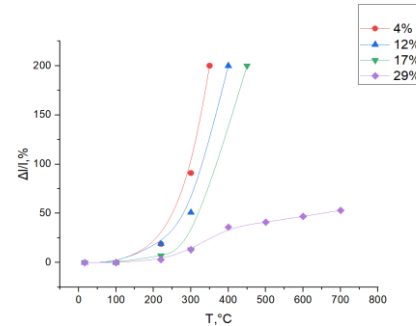


Fig. 3 – Dependence of the change in the length of the indentation cracks on the tempering temperature of the samples (Thermal shock)

$$R'' = \frac{K_{IC}(1-\nu)k}{aE}, \tag{3.1}$$

where  $K_{IC}$ ,  $\nu$ ,  $a$ ,  $k$ , and  $E$  are the toughness, Poisson's ratio, thermal expansion coefficient, thermal conductivity, and Young's modulus, respectively.

In [19], graphite content rise resulted in toughness improvement, which, together with the elasticity deterioration, increased the values of  $R''$ . However, as is evident from Table 3, in the presented materials, graphite addition led to toughness degradation approximately proportional to that of Young's modulus. Therefore, the nature of TSR improvement should be investigated additionally.

The manufactured composites microstructure consists of the HfB<sub>2</sub> matrix (the lightest areas on the SEM image, Fig. 4), silicon carbide inclusions (darker areas) with imbedded flake-like graphite particles (see Fig. 5).

However, structural non-uniformity was detected in the manufactured samples on the macroscopic scale. The mentioned non-uniformity was only observed in samples with the addition of silicon. On the surface, a well-defined separation line dividing the entire sample into inner and outer zones was clearly visible (Fig. 6).

Analysis of specific areas of the sample revealed slight differences in its composition, which could potentially lead to variations in its mechanical properties. As shown in Table 4, the analysis of the inner and outer parts (zone 2 and 1 in Fig. 7) indicates a certain difference in the quantity of Si atoms. Inside, its concentration is almost 4 at. % lower, which may result in a reduction in the microhardness of the inner layer.

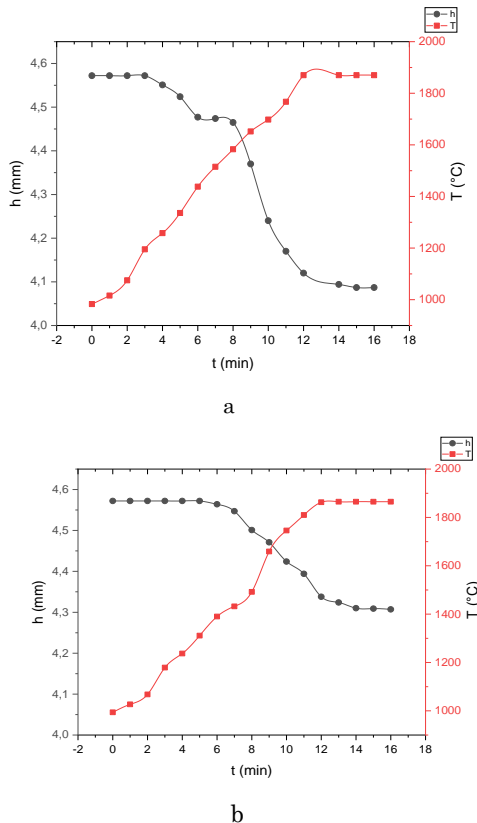
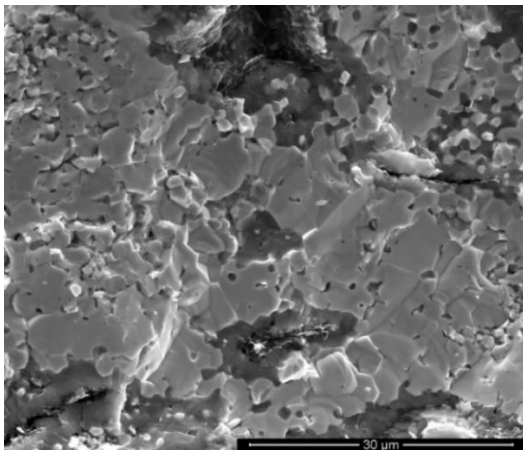
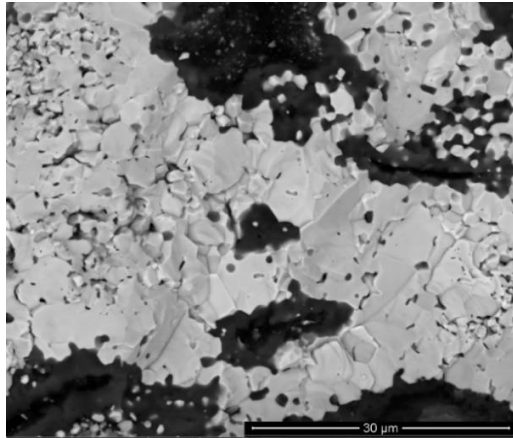


Fig. 2 – The sample heights ( $h$ ) and temperature ( $T$ ) evolution during the reactive (a) and non-reactive (b) hot pressing

**Table 3** – Graphite content, Young's modulus  $E$ , Microhardness HV, and toughness  $K_{1c}$  of sintered  $2HfB_2 + xSiC + (3 - x)C$  samples

Sample #	Graphite, vol.%	$\rho$ , g/sm <sup>3</sup>	$E^*$ , GPa	$H_v$ , GPa	$K_{1c}$ , MPa·m <sup>1/2</sup>
1	29	9.45	396	10	5.8
N1		8.32		7.5	5.2
2	23	9.06	416	15	5.3
3	17	8.88	437	16.1	6.3
4	12	8.47	454.5	17.3	5.8
N4		7.91		16.1	6.3
5	4	7.91	481.5	14.0	6.9
N5		7.13		18.9	6.6

\* Calculated based on the rule of mixtures



**Fig. 4** – SEM image (back-scattered and secondary electrons) of  $2HfB_2 + 1.5SiC + 1.5C$  (sample 4) fracture surface

EDS analysis also showed some zirconium. This is common for materials milled in a zirconium oxide container. The carbon atoms were not indicated due to the used EDX detector peculiarities.

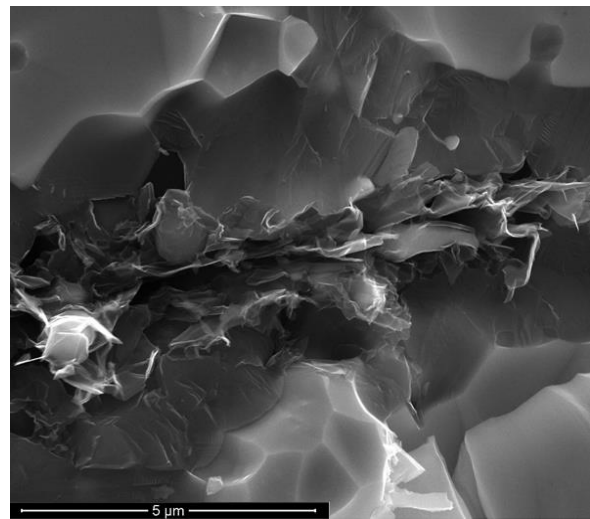


**Fig. 5** – Graphite inclusion in  $HfB_2-SiC$  matrix (sample 4).

**Table 4** – Analysis of At. % of individual elements in Zones 1 and 2

Element	At. #	Zone 1	Zone 2
		at. %	at. %
Boron	5	53.5	56
Hafnium	72	23.1	24.2
Silicon	14	19.8	15.9
Zirconium	40	3.6	3.9

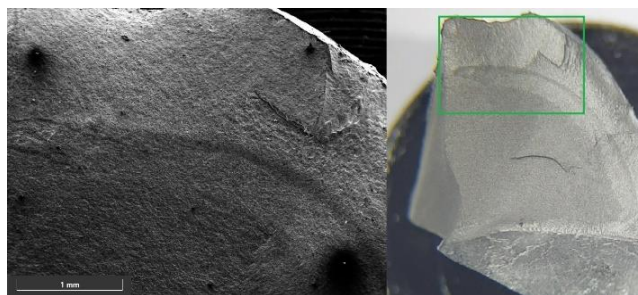


**Fig. 6** – SEM and optical images of sample 2 ( $2HfB_2 - 0.5SiC - 2.5C$ )

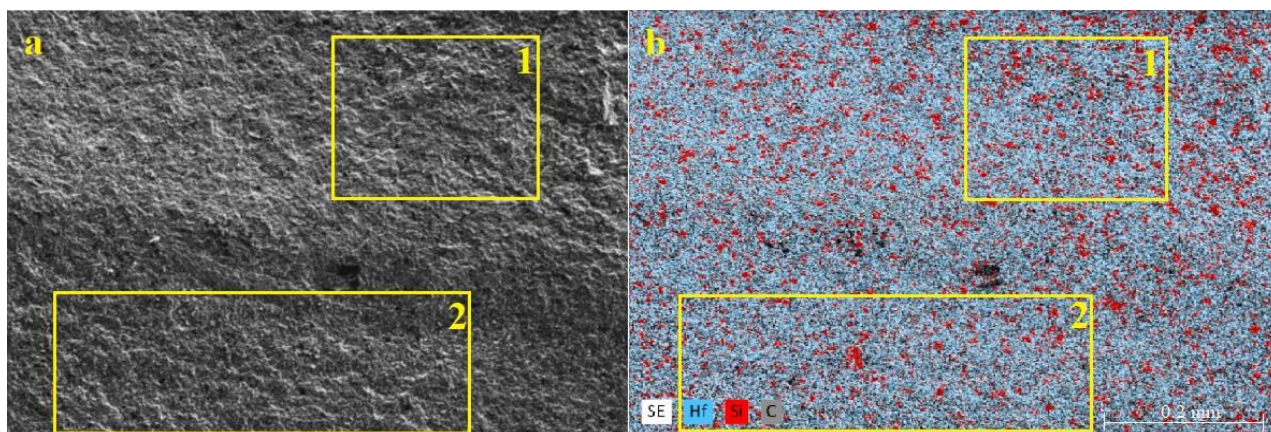


Fig. 7 – SEM (secondary electrons) (a), and EDS map (b) images of zones 1 and 2 of sample 2

#### 4. CONCLUSIONS

1. Hot pressing of HfC-B4C-Si powder mixtures at 1850 °C and 30 MPa for 4 minutes resulted in HfB<sub>2</sub>-SiC-C heteromodulus UHTCs.

2. The in-situ reactions intensified the charge densification and reduced the sintering time, which can be used for ultra-high-temperature ceramic manufacturing cost reduction.

3. Soft graphite plates formed during the reactive hot pressing procedure inside the stiff HfB<sub>2</sub>-based matrix impede crack propagation, improving the ceramic thermal shock resistance.

4. The delamination of reactively pressed materials with silicon-depleted inner areas of the samples was indicated.

#### ACKNOWLEDGMENT

This work has been supported by Ministry of Education and Science of Ukraine within project 24BΦ051-01 "Synthesis of biocompatible metal-ceramic composites to improve the wear resistance of medical instruments and titanium-based implants".

#### REFERENCES

- W.G. Fahrenholtz, G.E. Hilmas, *Scr. Mater.* **129**, 94 (2017).
- E. Wuchina, E. Opila, M. Opeka, W. Fahrenholtz, I. Talmy, *Electrochem. Soc. Interface* **16**, No 30, 30 (2007).
- D. Ni, Y. Cheng, J. Zhang, J.-X. Liu, J. Zou, B. Chen, H. Wu, H. Li, S. Dong, J. Han, X. Zhang, Q. Fu, G.-J. Zhang, *J. Adv. Ceram.* **11** No 1, 1 (2022).
- Ultra-High Temperature Ceramics: Materials for Extreme Environment Applications* (Ed. by W.G. Fahrenholtz) (Hoboken: Wiley: 2014).
- F.V. Harzand, S. Anzani, A. Babapoor, *Synth. Sinter.* **2** No 4, 186 (2022).
- M. Mallik, K.K. Ray, R. Mitra, *J. Eur. Ceram. Soc.* **31** No 1-2, 199 (2011).
- Q.-Q. Zhu, Y. Zhang, W.-M. Guo, S.-K. Sun, H.-T. Lin, *J. Am. Ceram. Soc.* **102** No 11, 6427 (2019).
- H. Liang, W. Sun, X. Li, H. Chen, S. Guan, P. Liu, Q. Wang, X. Li, D. He, F. Peng, *J. Alloy. Compd.* **808**, 151764 (2019).
- E. Simonenko, A. Kolesnikov, A. Chaplygin, M. Kotov, M. Yakimov, I. Lukomskii, S. Galkin, A. Shemyakin, N. Solovyov, A. Lysenkov, I. Nagornov, A. Mokrushin, N. Simonenko, N. Kuznetsov, *Int. J. Mol. Sci.* **24** No 17, 13634 (2023).
- M. Pavese, P. Fino, C. Badini, A. Ortona, G. Marino, *Surf. Coat. Technol.* **202**, No 10, 2059 (2008).
- W.G. Fahrenholtz, G.E. Hilmas, I.G. Talmy, J.A. Zaykoski, *J. Am. Ceram. Soc.* **5** No 90, 1347 (2007).
- O. Popov, J. Vleugels, E. Zeynalov, V. Vishnyakov, *J. Eur. Ceram. Soc.* **40** No 15, 5012 (2020).
- L. Silvestroni, D. Sciti, C. Melandri, S. Guicciardi, *J. Eur. Ceram. Soc.* **30** No 11, 2155 (2010).
- J. Zou, G.-J. Zhang, Y.-M. Kan, *J. Mater. Res.* **24** No 7, 2428 (2009).
- P. Zhou, P. Hu, X. Zhang, W. Han, *Scr. Mater.* **3** No 64, 276 (2011).
- W.-M. Guo, Y. You, G.-J. Zhang, S.-H. Wu, H.-T. Lin, *J. Eur. Ceram. Soc.* **35** No 6, 1985 (2015).
- S. Chornobuk, A. Popov, V. Makara, *J. Superhard Mater.* **31**, 86 (2009).
- O. Popov, V. Vishnyakov, *Adv. Appl. Ceram.* **116** No 2, 61 (2017).
- O. Popov, V. Vishnyakov, L. Poperenko, I. Yurglevych, T. Avramenko, A. Ovcharenko, *Ceram. Int.* **48** No 12, 17828 (2022).
- O. Popov, V. Vishnyakov, L. Fleming, M. Podgurskiy, L. Blunt, *ACS Omega* **7** No 2, 2205 (2022).
- O. Popov, A. Klepko, E. Lutsak, *Int. J. Refract. Met. Hard Mater.* **75**, 234 (2018).
- O. Popov, V. Vishnyakov, S. Chornobuk, I. Totsky, I. Plyushchay, *Ceram. Int.* **45** No 14, 16740 (2019).
- O. Popov, D. Shtansky, V. Vishnyakov, O. Klepko, S. Polishchuk, M. Kutzhanov, E. Permyakova, P. Teselko, *Nanomaterials* **12** No 8, 1379 (2022).
- S.J. Lee, E.S. Kang, S.S. Baek, D.K. Kim, *Surf. Rev. Lett.* **17** No 2, 215 (2010).
- S. Chornobuk, O. Popov, V. Makara, *Def. Fract. Mater.* No 11, 15 (2009).
- A.G. Evans, E.A. Charles, *J. Am. Ceram. Soc.* **59**, 371 (1976).
- O. Popov, T. Avramenko, V. Vishnyakov, *Mater. Today Commun.* **26**, 101756 (2021).
- T. Lu, N. Fleck, *Acta Mater.* **46** No 13, 4755 (1998).

## Реакційне гаряче пресування надвисокотемпературної кераміки $\text{HfB}_2\text{-SiC-C}$ з підвищеною стійкістю до термоудару

А. Овчаренко, В. Дібров, М. Семенко

*Київський національний університет імені Тараса Шевченка, 01601 Київ, Україна*

Виготовлення надвисокотемпературних керамік методом спікання вимагає підтримання високих температур порядку 1500 °С протягом декількох годин, тоді як у роботі був показаний альтернативний метод рівномірного формування відповідних мікрофаз, що в майбутньому здешевить процес виробництва. Сутність методу реакційного гарячого пресування полягає в запуску хімічної реакції за адіабатичної температури, що складає 60-80 % від температури плавлення прекурсорів, з додаванням зовнішнього тиску. Сукупність даних умов пришвидшує в рази процес ущільнення шихти. Шляхом реакційного гарячого пресування прекурсорів  $\text{HfC-B}_4\text{C-Si}$  при температурі 1850 °С та тиску 30 МПа протягом 4 хвилин було виготовлено гетеромодульну кераміку  $\text{HfB}_2\text{-SiC-C}$  з різним вмістом вуглецевих пластинок. Таким чином, мікротвердість синтезованої кераміки окремих хімічних складів досягала 17,3 ГПа, а тріщиностійкість 6,9 МПа/м<sup>2</sup>. Реакційно пресовані зразки було порівняно з нереакційно пресованими аналогічного складу. Дослідження характеристик кераміки було виконано методами рентгеноструктурного аналізу (XRD) та сканувальної електронної мікроскопії (SEM). Було встановлено, що включення вуглецю впливають на твердість кераміки  $\text{HfB}_2\text{-SiC}$  покращуючи при цьому стійкість до термоудару. Виявлено розшарування реакційно синтезованих зразків у зв'язку зі збідненням на кремній.

**Ключові слова:** Надвисокотемпературна кераміка, Реакційний синтез, Диборид гафнію, Стійкість до термоудару, XRD, SEM.